

ARTIFICIAL MUSCLES: STATE OF THE ART AND A NEW TECHNOLOGY

PETR KOCIS, RADEK KNOFLICEK

Brno University of Technology, Faculty of Mechanical Engineering,
Institute of Producing Machines, Systems and Robotics,
Brno, Czech Republic

DOI:10.17973/MMSJ.2017_02_2016100

e-mail: 126108@vutbr.cz

Pneumatic artificial muscles have been known since 1930s. Their advantage is in a simple design and good specific power [Madden 2004, Kocis 2016b]. However, the critical disadvantage is the requirement of an air compressor or a compressed air accumulator. This disadvantage disables the use of pneumatic artificial muscles in mobile robotics. In contrast to pneumatic artificial muscles dielectric elastomer actuators as basic units of artificial muscles are convenient for mobile robots propulsion [O'Brien 2012, Moghadam 2015]. We investigate a new design of pneumatic artificial muscles that can be powered by the energy of electrostatic field. This paper describes the design of a new artificial muscle technology and solves a behavior under small strains.

KEYWORDS

artificial muscle, pneumatic muscle, dielectric elastomer, electrostatics, actuator

INTRODUCTION

The theme of artificial muscles lies in a range of machine or robotic propulsion. It is a rather new type of propulsion exceeding the properties of conventional drives. Conventional drives, such as electromagnetic motors or combustion engines, are heavy and need transmission units, gear boxes and a cooling for the required performance.

The artificial muscles have a simple design which raises a low weight and good specific power. Depending on the technology of artificial muscles, most of them are able to produce high forces or torque with low revolutions or velocities, and thus they seem appropriate to be used in robotics [Madden 2004, Kocis 2016a].

1 CURRENT STATE OF RESEARCH

This review begins with a description of the artificial muscle design technology and sorts the technologies into two categories. The first category divides the technology by an energy source for a propulsion. This

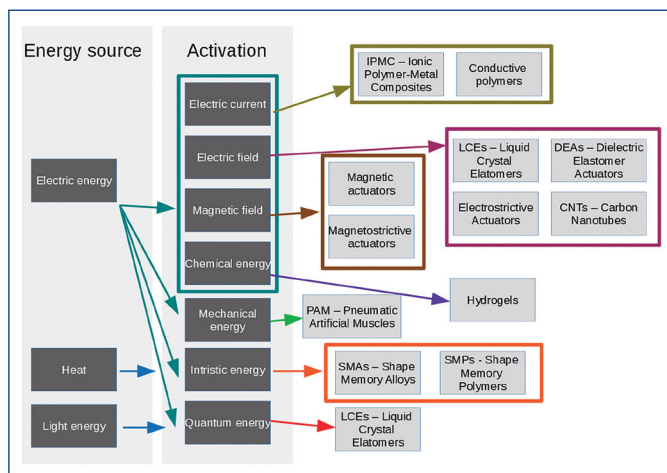


Figure 1. Distribution of artificial muscles technologies

includes electric power, heat and even a solar energy [Iamsaard 2014]. The second category divides technology by the activation of artificial muscles. As the Fig. 1 shows, most activation methods are dependent on electric power and some of them can be powered by more energy sources. Fig. 1 shows relationships between artificial muscles technologies, activation methods and a power source.

Pneumatic artificial muscles (PAMs) transform potential energy of pressured air into a mechanical movement and was developed by a Russian scientist Garasiev in 1930 [Kopečný 2009, Kocis 2016b]. The muscle consisted of rubber sleeve rounded by rims in several positions. The rims were connected by fibers.

The main point of PAM is ability of mimicking the structure and functioning mechanism of biological skeletal muscles through the pressurizing an air-tight tube surrounded by an inextensible mesh. When the internal space is pressurized, the tube expands in the radial direction and shortens in the axial direction, generating a pulling force to the external load. With this structure, the pneumatic muscle possesses multiple unique advantages, including simple structure, high power density, and similar elastic characteristics to biological skeletal muscles.

The best-known PAM is McKibben's muscle. The main feature of McKibben's PAM is a topology of a braid. Fibers of the braid cross each other and form pantographic units. Due to these pantographic units, the PAM has got a good deformation process [Kopečný 2009].



Figure 2. Braid of McKibben's PAM [Kopečný 2009]

Technology of smart memory alloys (SMA) or smart memory polymers (SMP) is the next currently used. SMAs and SMPs are activated by an intrinsic energy change, therefore, a power can be provided with electric energy or the heat. Basic element of SMA is a sheet or a wire of Ni-Ti alloys [Büttenbach 2001, Price 2007, Kocis 2016e]. As the element is heated, it changes its shape due to phase changes. Activation speed is dependent on heating and cooling period and it is usually slow. Also the effectivity is about 5 % [Anderson 2012].

Dielectric elastomer actuators (DEAs), electrostrictive actuators, liquid crystal elastomer actuators (LCEs) and carbon nanotube actuators (CNTs) are activated by an electrostatic field. LCEs and electrostrictive actuators respond to the electrostatic changes by conformational changes that induce bulk deformation. Nevertheless, these materials achieve low bulk changes in units of percentage. The DEAs basic units consist of three layers, as depicted in Fig. 2. Two external layers are used as conductive electrodes and they are made of a carbon grease or silver grease which both allow a planar deformation. These electrodes are charged by high voltage to generate the electrostatic field causing the electrodes attraction [Arora 2007, Brochu 2010, Maden 2004, Kocis 2016c, Kocis 2016d]. Electrode attraction causes the thickness shrinkage of the elastomer film which relaxes its tension in longitudinal axes. This relaxing results in the film elongation in longitudinal axes and the dielectric elastomer actuator causes a mechanical work. DEAs achieve a strain in dozens of percent. In [Madden 2004] it is noted that the activation pressures reach up to 7.7 MPa, active strains of over 380%, and response times of the order of milliseconds are reported. These parameters are strongly dependent on a used elastomeric material. The best results are achieved with three commercially available materials, as Dow Corning HS3 silicone, Nusil CF 19-2186 silicone, or 3M VHB 4910 acrylic [Madden 2004].

The effect of the electrostatic forces between unlike charges in each electrode are added to the compressive attraction between electrodes to produce the following expression:

$$p = \epsilon_0 * \epsilon_r * (U/t)^2 \quad (1)$$

where p is an electrostatic Maxwell's pressure, ϵ_r is the relative permittivity of the dielectric material, ϵ_0 is the permittivity of free space ($\epsilon_0 = 8,854 \times 10^{-12} \text{ F.m}^{-1}$), U is the voltage and t is the thickness of the elastomer film.

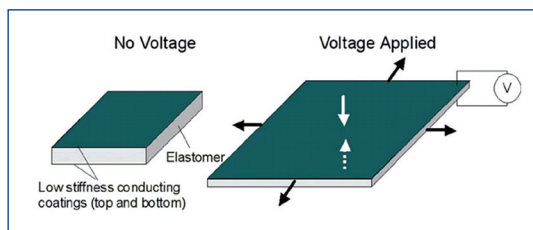


Figure 3. Schematic illustration of the DEA principle of operation [Madden 2004]

One of the best known applications of dielectric elastomer actuators is the Arm Wrestling Robot (Fig. 5) designed in Swiss Federal Laboratories for Materials Testing and Research [Kovacs 2007]. The equipment contains 256 rolled actuators (Fig. 4) with small diameters which are arranged in two groups according to the human agonist – antagonist muscle configuration in order to achieve an arm-like bidirectional rotation movement. Firstly, the active elastomer film is pre-stretched in both longitudinal and lateral directions. Secondly, the pre-stretched film is coated by carbon powder mixed with silicon oil to achieve conductivity of film surfaces. Two layers of elastomer are coated to prevent the sample from an electrical breakdown. Thirdly, the pre-stretched two elastomer layer is wrapped around the coil and sealed to enable the transmission of the external loads to the wrapped film [Kovacs 2007]. The core consists of a spring coil which maintains the film pre-stretched and a latex balloon preventing the dielectric film from any local stress concentrations. Other artificial muscle technologies are being incessantly laboratory developed. Technology of ionic polymer-metal composites is based on low electric potential between two metal electrodes, where the polymer electrolyte is placed. The polymer electrolyte is made of hydrophilic and low cross-linked polymers such as Nafion or Flemion [Madden

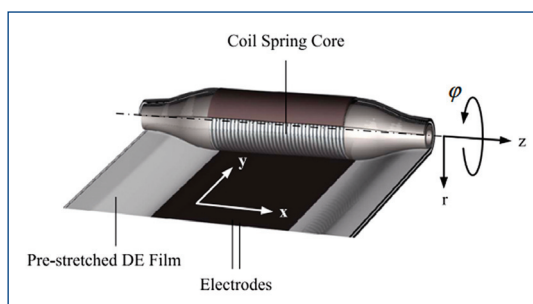


Figure 4. Schematic illustration of the rolled DEA [Kovacs 2007]



Figure 5. Representation of the Arm Wrestling Robot [Kovacs 2007]

2004], [Brochu 2010] to achieve low stiffness and a water permeability through the intrinsic structure. As the electrodes are activated, the nonuniform distribution of water produces swelling of one side of the actuator and contraction of the other, generating torque on the member and a bending motion [Brochu 2010].

Conducting polymers are conducting organic materials featuring conjugated structures [Tadesse 2009]. Electrochemically changing oxidation state leads to the addition or removal of charge from the polymer backbone and the flux of ions to balancing the charge. This ion flux causes swelling or contraction of the material. The insertion of ions between polymer chains appears to be primarily responsible for the dimensional changes, although the conformational changes of the backbone may also play a role [Madden 2004]. The changes in dimension lead to produce mechanical work.

Hydrogel actuators are water-filled polymers that reach significant bulk changes in response to the application of an external stimulus, such as pH, ionic concentration or electric field [Maden 2004, Kim 2013]]. The magnitude of the deformation and the response time of these hydrogel networks are affected by the molecular weight, the hydrophilicity of the polymer network, as well as the charge density of the polymer chains forming the polymeric network.

2 DESCRIPTION OF THE PROBLEM SITUATION

PAMs and DEAs are the most promising technologies at present. They both provide a good efficiency, a great response time and a good specific power [Madden 2004]. We investigate a new artificial muscle technology for a mobile robotic usage.

1. PAMs have good specific power [Madden 2004] but they are propelled by a compressed air accumulator or an air compressor. However, this equipment raises up a mass of whole propulsion.
2. DEAs necessarily need a frame to provide a prestrain of the dielectric film in both longitudinal and lateral direction. The frame occupies over 90 % mass of the artificial muscle [Anderson 2012], therefore reduces the specific power.

To solve the problem, it is necessary to design a pneumatic artificial muscle without a requirement of a pressured air source. It is also necessary to propose a frameless construction of DEA. These two requirements have lead to a new design of artificial muscle that differs from whole known artificial muscle technologies.

3 DESCRIPTION OF A NEW DESIGN – THE MENTAL MODEL

The new artificial muscle technology is entitled DEPAM (Dielectric Elastomer Pneumatic Artificial Muscle) due to its principle of operation:

- DEPAM consists of an active bag and two fittings at each end. In dependence on muscle geometry the fittings transfer a pulling or a pushing force into a driven mechanism and conclude a workspace of the muscle. The bag is made of a dielectric elastomer with high-voltage electrodes to activate the artificial muscle. The air-tight workspace of the artificial muscle is filled by pressured air. Overpressure in the workspace assures a strain of the bag in a longitudinal direction (which corresponds to the axial direction of the artificial muscle) and in a lateral direction (which corresponds to the radial direction of the artificial muscle). The ration between lateral strain and longitudinal depends on the muscle geometry.
- Electrodes attraction caused by charged electrodes relaxes a tension in longitudinal and lateral direction of the elastomeric film. As the film is relaxed, intrinsic pressure leads to volume change of DEPAM that induces mechanical work. Discharging electrodes returns the DEPAM into the initial state.

4 MATERIALS AND METHODS

The new technology of artificial muscles described in previous chapter forms a basis for geometry models. DEPAM can be realized by various geometric models, nevertheless, only the cylindrical geometry will be solved in this paper. The cylindrical geometry is defined by these conditions:

- The active bag of DEPAM has a tubular shape. with constant strain in radial direction.
- External surface of the bag is supplied by inextensible fibres to avoid expanding the bag in radial direction.
- Magnitude of lateral strain is limited by the inextensible fibers, thus the artificial muscle preserves a constant radius.
- As the film is relaxed, intrinsic pressure leads of the bag in axial direction.
- Schematic illustration of cylindrical geometry is depicted in Fig. 6.

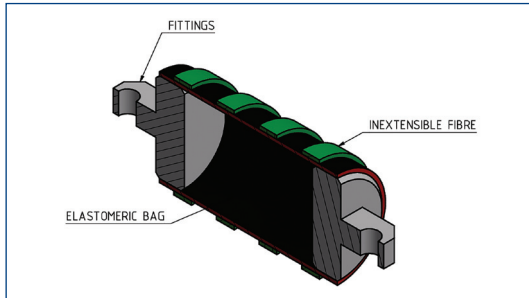


Figure 6. Schematic illustration of cylindrical geometry of DEPAM

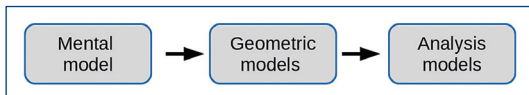


Figure 7. Process of DEPAM development

The new technology of artificial muscles described in previous chapter is defined as a mental model and it is necessary to perform a verification. The verification is based on the cylindrical geometry and follows the process depicted in Fig. 7. Aims of verification are:

- to describe a functionality of DEPAM,
- to determine a relationships between input energy and external work.

Verification of the mental model will be performed by an analysis model of cylindrical geometry of DEPAM. This analysis model has this conditions:

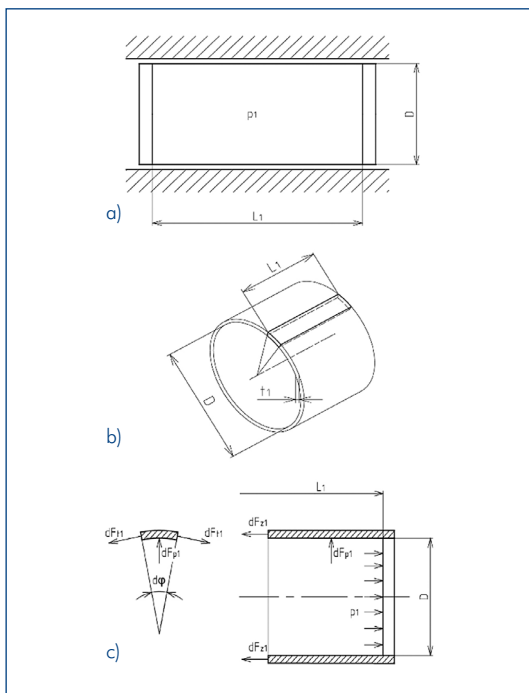


Figure 8. Analysis of DEPAM in initial state: a) geometry of DEPAM, b) elementary volume, c) loads and stresses of DEPAM in initial state.

1. The analysis model solves a stress in the bag of the muscle.
2. The condition stated in 1 deals with a triaxial state of stress and strains in three axes identical with the axes of stress.
3. The intention of the bag is located in the area of linear behavior of material and thus it is solved for a low strains and allows generalized Hooke's Law use.
4. The analysis model is solved for low operation frequencies $f \ll 1$ Hz.
5. In pressured air in workspace of DEPAM the isothermic transformation processes according to condition 4.
6. The function of inextensible fibers is replaced with a sliding constrain in the analysis model.

The analysis model is defined for two cases; the first case without high-voltage electrodes activation and the second case with high-voltage electrodes activation. Case 1 is an initial state and is characterized by zero values of external forces. Case 2 is activated state and is characterized by process of DEPAM elongation in axial direction.

To determine relationships, the geometric dependences have to be determined. A geometry of DEPAM is depicted in Fig. 8a. Fig. 8b depicts an elementary volume of the bag in initial state and Fig. 8c depicts loads and a stress of the elementary volume in initial state. For this state $\sigma_{r1} = 0$ MPa and $\epsilon_{r1} = 0,05$ are applied.

For generalized Hooke's Law:

$$\epsilon_{r1} = \frac{1}{E} \cdot [\sigma_{r1} - \mu \cdot (\sigma_{z1} - \sigma_{t1})] \quad (2)$$

$$\epsilon_{t1} = \frac{1}{E} \cdot [\sigma_{t1} - \mu \cdot (\sigma_{z1} - \sigma_{r1})] \quad (3)$$

$$\epsilon_{z1} = \frac{1}{E} \cdot [\sigma_{z1} - \mu \cdot (\sigma_{t1} - \sigma_{r1})] \quad (4)$$

where ϵ_{r1} is the strain in radial direction in case 1 [-], ϵ_{t1} is the strain in tangential direction in case 1 [-], ϵ_{z1} is the strain in axial direction in case 1 [-], E is the tension modulus [MPa], σ_{r1} is the stress in radial direction in case 1 [MPa], σ_{t1} is the stress in tangential direction in case 1 [MPa], σ_{z1} is the stress in axial direction in case 1 [MPa] and μ is Poisson's ratio [-].

An equilibrium of loads in radial direction in case 1 is described by equations (5) – (8):

$$-2 \cdot F_{t1} \cdot \sin \frac{d\varphi}{2} + dF_{p1} = 0 \quad (5)$$

$$-2 \cdot F_{t1} \cdot \frac{d\varphi}{2} + dF_{p1} = 0 \quad (6)$$

$$\sigma_{t1} \cdot t_1 \cdot L_1 \cdot d\varphi = p_1 \cdot L_1 \cdot \frac{D}{2} \cdot d\varphi \quad (7)$$

$$\sigma_{t1} = p_1 \cdot \frac{D}{2 \cdot t_1} \quad (8)$$

where F_{t1} is the tangential force in case 1 [N], F_{p1} is the intrinsic pressure force in case 1 [N], $d\varphi$ is the angle of the elementary volume [rad], p_1 is the intrinsic pressure in case 1 [MPa], L_1 is the length of the active part of DEPAM in case 1 [mm], t_1 is the thickness of the elastomeric film in case 1 [mm] and D is the internal diameter of the bag.

An equilibrium of loads in axial direction in case 1 is described by equations (9) – (11):

$$F_{z1} = p_1 \cdot \frac{\pi \cdot D^2}{4} \quad (9)$$

$$\sigma_{z1} \cdot t_1 \cdot \pi \cdot D = p_1 \cdot \frac{\pi \cdot D^2}{4} \quad (10)$$

$$\sigma_{z1} = p_1 \cdot \frac{D}{4 \cdot t_1} \quad (11)$$

where F_{z1} is the force in axial direction in case 1 [N].

Equations of compatibility:

$$L_1 = L \cdot (1 + \varepsilon_{z1}) \quad (12)$$

$$t_1 = t \cdot (1 + \varepsilon_{r1}) \quad (13)$$

where L is the length of unextended elastomeric film [mm] and t is the thickness of unextended elastomeric film.

Fig. 9a depicts the activated state. Fig. 9b and Fig. 9c depict an elementary volume of DEPAM's bag in activated state. For this state $\sigma_{r2} = 0$ MPa and $\varepsilon_{r1} = \varepsilon_{r2} = 0,05$ are applied.

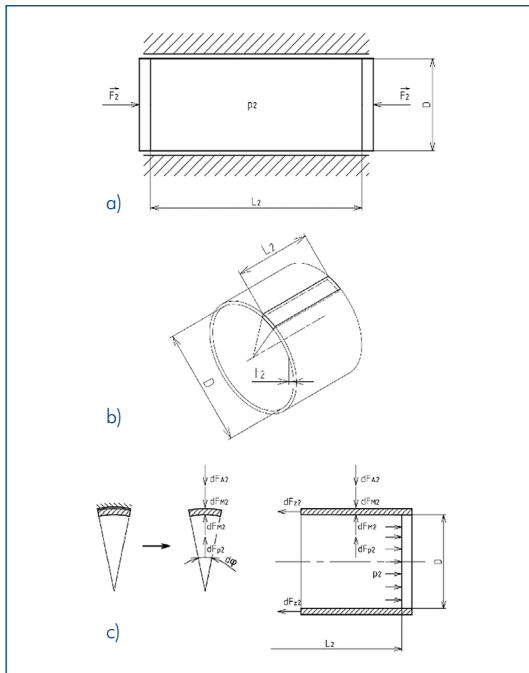


Figure 9. Analysis of DEPAM in activated state: a) geometry of DEPAM, b) elementary volume, c) loads and stresses of DEPAM in activated state.

For generalized Hooke's Law:

$$\varepsilon_{r2} = \frac{1}{E} \cdot [\sigma_{r2} - \mu \cdot (\sigma_{z2} - \sigma_{t2})] \quad (14)$$

$$\varepsilon_{t2} = \frac{1}{E} \cdot [\sigma_{t2} - \mu \cdot (\sigma_{z2} - \sigma_{r2})] \quad (15)$$

$$\varepsilon_{z2} = \frac{1}{E} \cdot [\sigma_{z2} - \mu \cdot (\sigma_{t2} - \sigma_{r2})] \quad (16)$$

where ε_{r2} is the strain in radial direction in case 2 [-], ε_{t2} is the strain in tangential direction in case 2 [-], ε_{z2} is the strain in axial direction in case 2 [-], σ_{r2} is the stress in radial direction in case 2 [MPa], σ_{t2} is the stress in tangential direction in case 2 [MPa], and σ_{z2} is the stress in axial direction in case 2 [MPa].

An equilibrium of loads in radial direction in case 2 is described by equations (17) – (19):

$$dF_{p2} + dF_{M2} = \sigma_{r2} \cdot L_2 \cdot \frac{D}{2} \cdot d\varphi \quad (17)$$

$$p_2 \cdot L_2 \cdot \frac{D}{2} + dF_{M2} = \sigma_{r2} \cdot L_2 \cdot \frac{D}{2} \cdot d\varphi \quad (18)$$

$$dF_{M2} = L_2 \cdot \frac{D}{2} \cdot d\varphi \quad (19)$$

where F_{p2} is the intrinsic pressure force in case 2 [N], F_{M2} is the force of Maxwell's (electrostatic) pressure in case 2 [N], p_2 is the intrinsic pressure in case 2 [MPa], L_2 is the length of the active part of DEPAM in case 2 [mm], and σ_{r2} is the stress in radial direction in case 2 [MPa].

An equilibrium of loads in axial direction in case 2 is described by equations (20) and (21)

$$F_2 + \sigma_{z2} \cdot t_2 \cdot \pi \cdot D - p_2 \cdot \frac{\pi \cdot D^2}{4} = 0 \quad (20)$$

$$F_2 = p_2 \cdot \frac{\pi \cdot D^2}{4} - \sigma_{z2} \cdot t_2 \cdot \pi \cdot D \quad (21)$$

where F_2 is the external force [N], σ_{z2} is the stress in axial direction in case 2 [MPa], and t_2 is the thickness of elastomeric film in case 2 [mm].

Equations of compatibility:

$$L_2 = L \cdot (1 + \varepsilon_{z2}) \quad (22)$$

$$t_2 = t \cdot (1 + \varepsilon_{r2}) \quad (23)$$

and additional equations:

$$p_{M2} = \varepsilon_0 \cdot \varepsilon_r \cdot \left(\frac{U}{t_2}\right)^2 \quad (24)$$

$$dF_{M2} = p_{M2} \cdot L_2 \cdot \frac{D}{2} \cdot d\varphi \quad (25)$$

$$F_{M2} = p_{M2} \cdot L_2 \cdot \pi \cdot D \quad (26)$$

$$F_{M2} = L_2 \cdot \pi \cdot D \cdot \varepsilon_0 \cdot \varepsilon_r \cdot \left(\frac{U}{t_2}\right)^2 \quad (27)$$

Equation (24) is analogy of equation (1), equation (25) is analogy of Pascal's Law in geometry element in case 2 and equations (26) and (27) are modifications, p_{M2} is Maxwell's (elektrostatic) pressure [MPa], ε_0 is the permittivity of free space [F.m⁻¹], ε_r is the relative permittivity of the dielectric material [-], and U is the voltage [V].

In connection with isothermic expansion of the pressured air:

$$p_1 \cdot V_1 = p_2 \cdot V_2 \quad (28)$$

$$p_1 \cdot L = p_2 \cdot L_2 \quad (29)$$

where V_1 is the volume of the workspace in case 1 [mm³] and V_2 is the volume of the workspace in case 2 [mm³].

5 RESULTS AND DISCUSSION

Base on the analysis model, the process of the external force F_2 and the electrostatic force F_{M2} can be found. Due to the equation (27) it was

found that the voltage U is dependent on the length L_2 accordingly to equation 30:

$$U = k_1 \cdot L_2^{\left(\frac{3}{2}\right)} + k_2 \quad (30)$$

where k_1 and k_2 are the coefficients that are dependent on material and dimensional characteristics. The external work F_2 is inversely proportional on the length L_2 , so the curve plotted in figure 10 is part of a hyperbola. Then the equation can be defined as:

$$F_2 = \frac{k_3}{L_2} + k_4 \quad (31)$$

where k_3 and k_4 are the coefficients that are dependent on a material, characteristics dimensional characteristics and external conditions. The equations (30) and (31) are the characteristic equations of DEPAM. These dependencies are important for DEPAM control.

An example for analysis model can be made. Tab. 1 contains input parameters for the analysis model. Material parameters are chosen according to [Bozlar 2012]. Fig. 10 depicts a dependence of the

Geometric and material parameters					
Tension modulus E	0,25 [Bozlar 2012]	MPa	Strains:		
Internal diametr of the bag D	5	mm	ϵ_{r1}	0,1	–
Bag thickness t_1	0,15	mm	ϵ_{r2}	0,1 – 0,3	–
Length of unextended elastomeric film L	50	mm	Stresses:		
Poisson's constant μ	0,33	–	σ_{r1}	0	Mpa
Permittivity of free space ϵ_0	8,85419E-12	–	σ_{r2}	0	Mpa
Relative permittivity ϵ_r	3	–			

Table 1. Input parameters for the analysis model

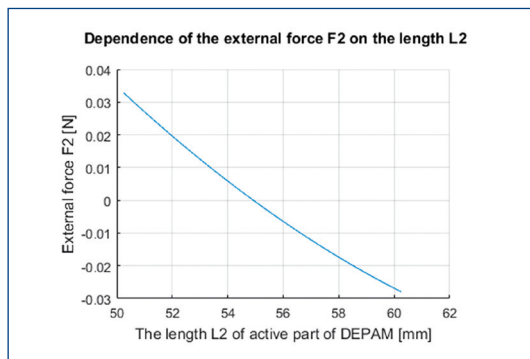


Figure 10. Dependence of the external force F_2 on the length L_2

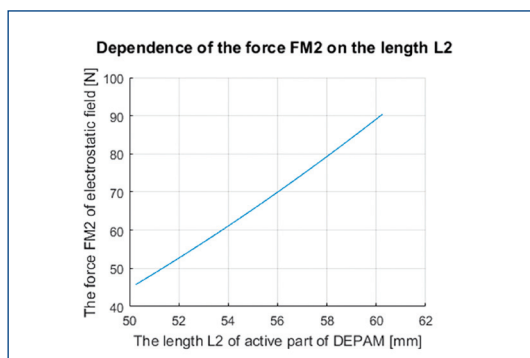


Figure 11. Dependence of the force F_{M2} on the length L_2

external force F_2 and Fig. 11 depicts a dependence of the electrostatic force F_{M2} on the length L_2 .

Although it is not clearly visible in the graphs, it was found that F_{M2} proportionally grows on increasing thickness t_2 and quadratically grows on increasing length L_2 . The thickness t_2 is linearly dependent on the length L_2 . The results would be more visible, if the analysis model was made for large strains.

CONCLUSIONS

This paper has described a new technology of artificial muscles entitled DEPAM (Dielectric Elastomer Pneumatic Artificial Muscle). The basic direction for following research was shown with the mental model. Behavior of the external force and input voltage were computed with analysis model for cylindrical geometry. Nevertheless, this was only the first step in the development a new artificial muscles technology. In the next steps of the research various geometric models should be created and analysed and the optimal solution should be evaluated. For detecting a real behavior for large deformations of the optimal solution a real sample of DEPAM should be realized. It is important to note that this technology is able to start a revolution in mobile robotics propulsion.

ACKNOWLEDGEMENTS

This work has been supported by Brno University of Technology, Faculty of Mechanical Engineering, Czech Republic (Grant No. FSI-S-14-2401).

REFERENCES

- [Anderson 2012] Anderson, I.A., et al. Multi-functional dielectric elastomer artificial muscles for soft and smart machines. Journal of Applied Physics, 2012, Vol.112., No.4.
- [Arora 2007] Arora, S., et al. Dielectric elastomer based prototype fiber actuators. Sensors and Actuators, A: Physical, 2007, Vol.136, No.1, pp. 321-328.
- [Bozlar 2012] Bozlar, M., et al. Dielectric elastomer actuators with elastomeric electrodes. Applied Physics Letters, 2012, Vol.101, No.9.
- [Brochu 2010] Brochu, P. and Pei, Q. Advances in dielectric elastomers for actuators and artificial muscles. Macromolecular Rapid Communications, 2010, Vol.31, No.1, pp. 10-36.
- [Büttgenbach 2001] Büttgenbach, S., et al. Shape memory micro-actuators. Microsystem Technologies, 2001, Vol.7, No.4, pp. 165-170.
- [Iamsaard 2014] Iamsaard, S., et al.. Conversion of light into macroscopic helical motion. Nature Chemistry, 2014, Vol.6, No.3, pp. 229-235.
- [Kim 2013] Kim, O., et al. 2013, Fast low-voltage electroactive actuators using nanostructured polymer electrolytes. Nature Communications, 2013, Vol.4.
- [Kocis 2016a] Kocis, P. and Knoflicek, R. Artificial Muscles, Part 1: History and Introduction (in Czech). ISSN 1212-2572. Praha: MM Průmyslové spektrum, 2016.
- [Kocis 2016b] Kocis, P. and Knoflicek, R. Artificial Muscles, Part 2: Pneumatic Muscles (in Czech). ISSN 1212-2572. Praha: MM Průmyslové spektrum, 2016.
- [Kocis 2016c] Kocis, P. and Knoflicek, R. Artificial Muscles, Part 3: Dielectric Elastomers – First Section (in Czech). ISSN 1212-2572. Praha: MM Průmyslové spektrum, 2016.
- [Kocis 2016d] Kocis, P. and Knoflicek, R. Artificial Muscles, Part 3: Dielectric Elastomers – Second Section (in Czech). ISSN 1212-2572. Praha: MM Průmyslové spektrum, 2016.
- [Kocis 2016e] Kocis, P. and Knoflicek, R. Artificial Muscles, Part 4: Magnetic Artificial Muscles And SMAs (in Czech). ISSN 1212-2572. Praha: MM Průmyslové spektrum, 2016.
- [Kopečný 2009] Kopečný, L. Modelling and Using of McKibben Pneumatic Muscle. Brno: VUT Brno, 2009.
- [Kovacs 2007] Kovacs, G., et al. An arm wrestling robot driven by dielectric elastomer actuators. Smart Materials and Structures, 2007, Vol.16., No.2., pp S306-S317.

[Madden 2004] Madden J. D. W., et al. Artificial Muscle Technology: Physical Principles and Naval Prospects. IEEE Journal of Oceanic Engineering, July 2004, Vol.29, No.3., pp 706-728.

[Moghadam 2015] Moghadam, A.A.A., et al. Development of a novel soft parallel robot equipped with polymeric artificial muscles. Smart Materials and Structures, 2015, Vol.24, No.3.

[O'Brien 2012] O'Brien, B.M. and Anderson, I.A. An artificial muscle ring oscillator. IEEE/ASME Transactions on Mechatronics, 2012, Vol.17, No.1, pp. 197-200.

[Price 2007] Price, A.D., et al. Design and control of a shape memory alloy based dexterous robot hand. Smart Materials and Structures, 2007, Vol.16, No.4, pp. 1401-1414.

[Tadesse 2009] Tadesse, Y., et al. Synthesis and cyclic force characterization of helical polypyrrole actuators for artificial facial muscles. Smart Materials and Structures, 2009, Vol.18, No.8.

CONTACTS

Ing. Petr Kocis

Brno University of Technology

Faculty of Mechanical Engineering

Institute of Producing Machines, Systems and Robotics

Technická 2896/2, 616 69 Brno, Czech Republic

tel.: +420 730 662 442

e-mail: 126108@vutbr.cz